Journal of Ceramic Processing Research. Vol. 19, No. 4, pp. 316~320 (2018)

J O U R N A L O F
Ceramic Processing Research

Electrocaloric properties of $K(Ta_{0.6}Nb_{0.4})O_3/SrTiO_3$ double layer thin films using metal alkoxides

Min-Su Kwon, Sung-Gap Lee* and Kyeong-Min Kim
Dept. of Materials Engineering and Convergence Technology, RIGET, Gyeongsang National University, Jinju 52828, Korea

In this study, KTN/STO thin films were fabricated on $Pt/Ti/SiO_2/Si$ substrate, as a buffer layer, and their structural and electrical properties were measured according to the number of STO coatings and investigated its applicability to electrocaloric materials. KTN/STO thin films showed a polycrystalline KTN XRD peaks with a pyrochlore phase. However, dependence on the number of STO coatings and pyrochlore phase was not observed. The average grain size was about 80~90 nm, the average thickness of 6-coated KTN thin film was about 320 nm, and the average thickness of the STO thin film coated once was about 50-55 nm. Saturation polarization of $K(Ta_{0.6}Nb_{0.4})O_3/SrTiO_3$ thin films was 24.5 $\mu C/cm^2$. Electrocaloric temperature change ΔT of $K(Ta_{0.6}Nb_{0.4})O_3$ thin film showed the maximum value of 3.14 ^oC at around 76 ^oC under a high electric field of 332.9 kV/cm.

Key words: Electrocaloric effect, KTN, Seeding layer, Hysteresis loop, Sol-gel method.

Introduction

Cooling devices, which have been in common use for a long time, used the vapor-compression refrigeration cycle as used in refrigerators. However, such a cooling device has a disadvantage in that it cannot be applied to a small and fine electronic device cooling device such as a computer or a communication device due to difficulty in miniaturization and vibration. Recently, many studies have been conducted on thermoelectric, magnetocaloric and electrocaloric effect as a next generation cooling device [1]. Particularly, the electrocaloric (EC) effect is attracting attention due to the possibility of miniaturization and the advantage of high energy conversion efficiency. EC effect, which is a reverse effect of the pyroelectric effect, is a phenomenon in which the temperature change (ΔT) of a material occurs due to the change of electric dipoles and entropy by application of an electric field. Many studies have been conducted on thin films or bulk of ferroelectric $Pb(Zr,Ti)O_3$ or $BaTiO_3$ ceramics [2, 3].

Alkaline niobate materials have been studied as lead-free ferroelectric materials to replace $Pb(Zr,Ti)O_3$ in environmental aspects. Especially, $K(Ta_xNb_{1-x})O_3$ (KTN) ceramics forms a solid solution over the entire composition range of x, such as $Pb(Zr,Ti)O_3$ or $BaTiO_3$ and it can control the crystal structure and the Curie temperature on the ferroelectric-paraelectric phase according to the change on Ta/Nb composition [4]. KTN materials are attracting much attention due to their excellent ferroelectric, dielectric, photo refractive, electrooptic and non-linear optical properties [5, 6]. However, KTN has a disadvantage that it is difficult to obtain high quality crystals having stoichiometric composition due to high volatility of K ion. KTN thin films have been fabricated by various methods such as pulsed laser deposition, sputtering, and sol-gel method [7, 8]. The crystallinity and the orientation of KTN thin films have dependence on the fabrication conditions and substrate of the films, and the epitaxial and high orientation films were prepared by $SrTiO_3$, MgO, Al_2O_3 substrates by various preparation techniques [9].

In this study, KTN and $SrTiO_3$ (STO) coating solutions were fabricated by using sol-gel method which can control precise composition, and STO films with excellent crystallographic and thermodynamic properties were deposited on Si substrates by spin coating method. The structural and electrical properties of KTN thin films were measured according to the number of coatings of STO films and investigated its applicability to electrocaloric materials.

Experimental

KOC_2H_5, $Ta(OC_2H_5)_5$ and $Nb(OC_2H_5)_5$ were used as starting materials and $CH_3OCH_2CH_2OH$ as the solvent and precursor solution with KTN (60/40) composition was prepared by sol-gel method. The solution synthesis procedure was conducted in a N_2 atmosphere because metal alkoxides are very sensitive to moisture. Potassium was first dissolved in 2-MOE, then mixed with the 2-MOE solution of tantalum ethoxide and niobium ethoxide which was prepared beforehand

*Corresponding author:
Tel : +82-55-772-1687
Fax: +82-55-772-1689
E-mail: lsgap@gnu.ac.kr

according to the composition ratio, and then stirred. The mixed solution was refluxed for 24 hrs. STO solution was prepared by sol-gel method using $Sr(CH_3COO)_2$, $Ti(OC_4H_9)_4$ as reagent and CH_3COOH as a solvent. The STO lower layer was fabricated by changing the number of coatings on $Pt(111)/Ti/SiO_2/Si$ substrate by 0, 1, 2 and 4 times by spin coating method. Then, KTN thin films were coated 6 times on the STO lower layer to fabricate the KTN/STO double layer structure thin film. KTN and STO coating solutions were spin-coated at 3500 rpm for 30 sec, followed by a drying step at 200 °C for 20 min in air to form gel films and a conducting pyrolysis step at 400 °C for 20 min to remove the organic materials, and finally annealing temperatures of STO and KTN films were 700 °C and 750 °C, respectively. The microstructure of the resultant thin film was observed by the field-emission scanning electron microscope (FE-SEM, Philips XL30S FEG) and crystal structure was determined by X-ray diffraction (XRD) analysis. A Pt-upper electrode with a diameter of 500 μm was deposited on the film by dc sputtering method in order to measure the electrical properties. Polarization hysteresis loops were analyzed using a ferroelectric test system (RT66B, NM, USA).

Results and Discussion

Fig. 1 shows XRD patterns of KTN/STO thin films according to the number of STO coatings. Generally, substrates such as STO and MgO are used to obtain a high quality KTN single phase thin film. All KTN/STO thin films showed a polycrystalline KTN XRD peaks with a pyrochlore phase. However, dependence on the number of STO coatings and pyrochlore phase was not observed. This is due to the formation of $K_2Ta_2O_6$ (JCPDS 35-1464) pyrochlore phase because the strong covalent bonding property of Nb ion and volatilization of K ion during specimen sintering [14]. Fig. 1(b) shows the XRD patterns around $2\theta = 45°$ to observe the effect of STO thin film on KTN crystal growth. In the case of KTN/STO films, the diffraction peaks slightly shifted to low angles and no dependence was observed on the number of coatings. It is considered that the STO lower layer served as a seed layer for KTN crystallization because STO (a = 0.3905 nm) and KTN (a=0.3990 nm) have the same perovskite crystal structure and good lattice matching properties [10].

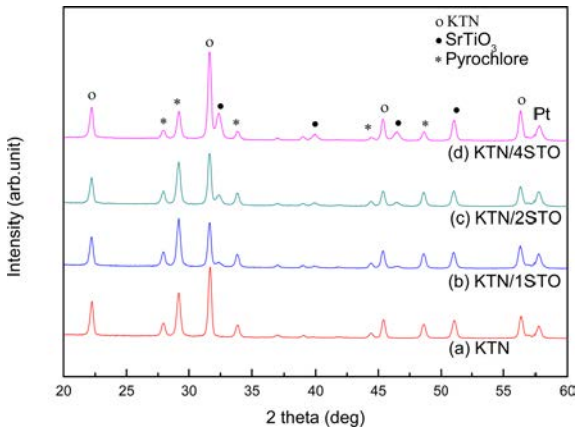

Fig. 1. XRD patterns of KTN/STO thin films according to the number of STO coatings.

Fig. 2 shows the surface and cross-sectional microstructures of KTN/STO thin films coated with two times STO films. It showed uniform grain size and flat surface microstructure, and the average grain size was about 86.5 nm. The average thickness of KTN thin films was about 320 nm, and the average thickness of the one time coated STO thin film was about 50-55 nm. The interface between KTN layer and STO layer was not observed, and micro-pores due to K ion volatilization were observed.

Fig. 3 shows dielectric constant and dielectric loss of KTN/STO thin films with the number of STO coatings and temperature. As the temperature increased, dielectric constant gradually decreased and saturates at about 40°C. And, dielectric constant tended to decrease with increasing the number of STO film coating times. In general, Curie temperature of STO material is about 110 °K and relative dielectric constant at room temperature is about 285 [11]. According to R. E. Newnham's report [12], when two phases with different permittivity are connected in series, the average dielectric constant is expressed as

$$1/\overline{\varepsilon_{\delta\delta}} = 1_{\upsilon}/1_{\varepsilon_{\delta\delta}} + {}^{2}\upsilon/{}^{2}\varepsilon_{\delta\delta} \quad (1)$$

where $\overline{\varepsilon_{\delta\delta}}$ is the average dielectric constant of a double layer film, and ${}^{1}\varepsilon_{\delta\delta}$ and ${}^{1}\upsilon$ are dielectric constant and volume of one phase, and ${}^{2}\varepsilon_{\delta\delta}$ and ${}^{2}\upsilon$ are dielectric constant and volume of the two phase, respectively.

Dielectric constants of the two-layered KTN/STO

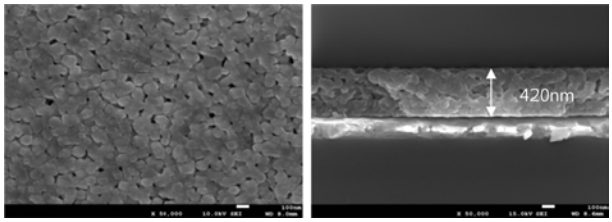

Fig. 2. Surface and cross-sectional microstructures of KTN/STO thin films coated with two times STO films.

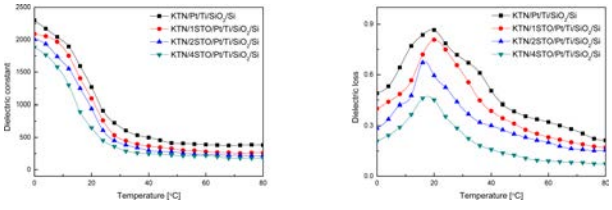

Fig. 3. Dielectric constant and dielectric loss of KTN/STO thin films with the number of STO coatings and temperature.

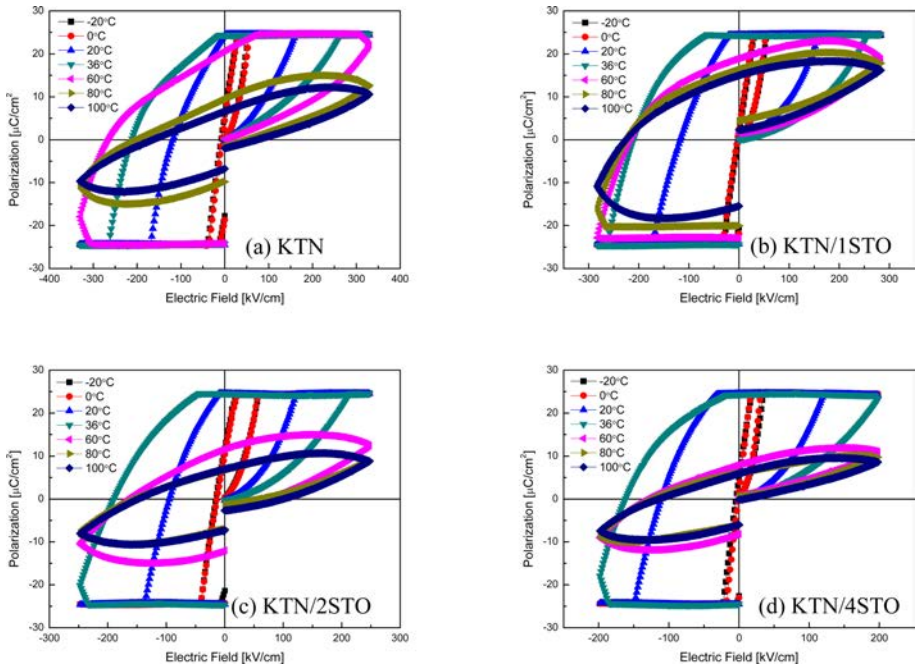

Fig. 4. Hysteresis loops of KTN/STO thin films according to the number of STO coatings.

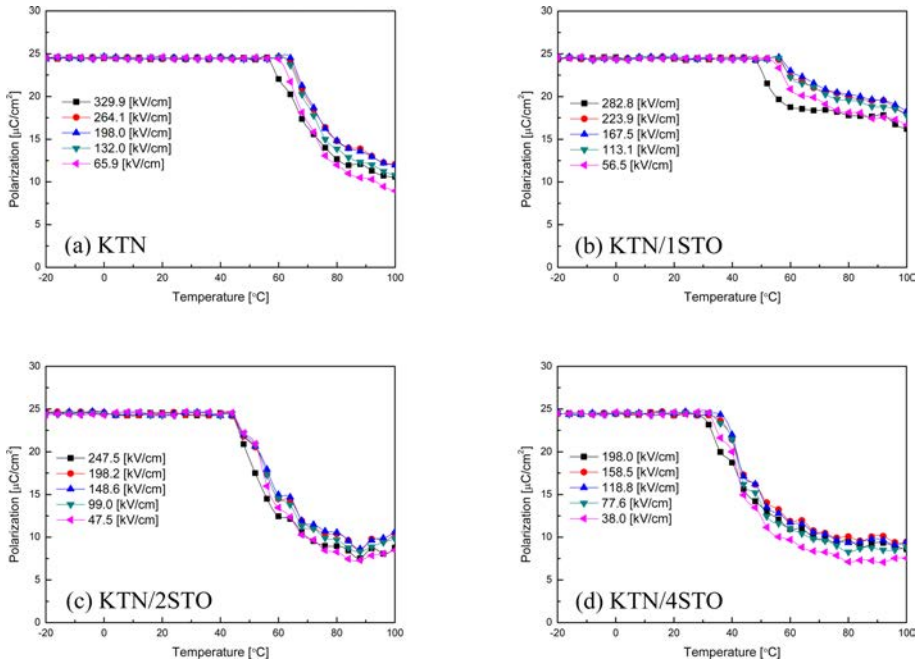

Fig. 5. Saturation polarization of KTN/STO thin films according to the number of STO coatings and temperature.

thin films are larger than those calculated from Eq. (1). This is because the lower STO layer affects the crystallization of the upper KTN thin films, as shown in Fig. 1, resulting in the formation of secondary phase between KTN film and STO film interface [13].

Fig. 4 shows hysteresis loops of KTN/STO thin films according to the number of STO coatings. The dependence of remanent polarization on the number of coatings of STO was not observed. It is considered that when ferroelectric phase and paraelectric phase are mutually bonded, the dipole moment of paraelectric phase is rearrangement by the ferroelectric phase dipoles [14]. Remanent polarization began to decrease around 60 ºC, and remanent polarization decreased with increasing the number of STO film coatings. It is considered that the dipole moment arrays of STO layer induced by KTN ferroelectric phase are easily disordered by the external thermal energy as the number of STO coating increases.

Fig. 5 shows saturation polarization of KTN/STO thin films according to the number of STO coatings and temperature. Saturation polarization sharply decreased in

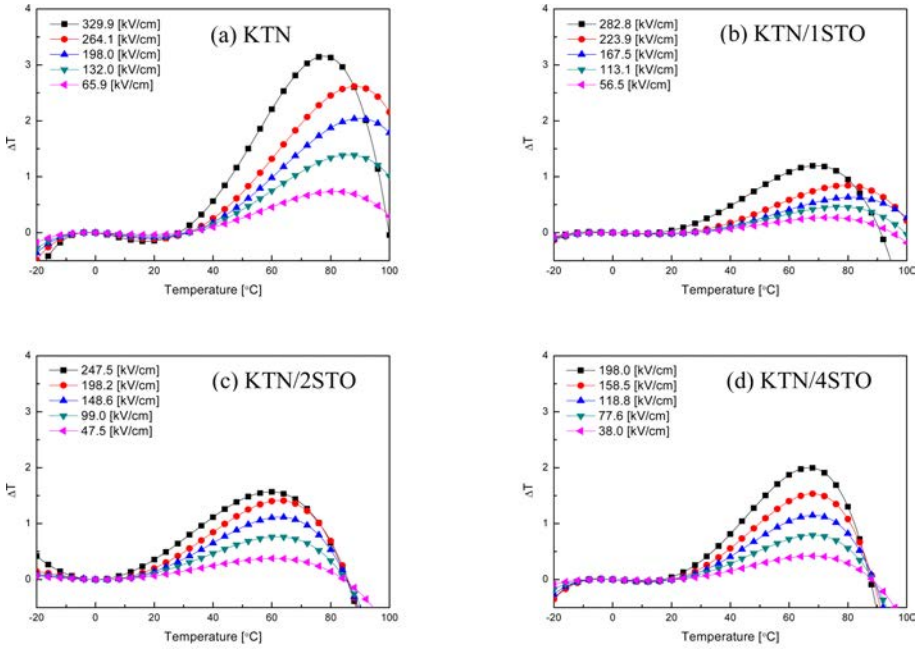

Fig. 6. Electrocaloric temperature change ΔT of KTN/STO thin films according to the number of STO coatings.

the vicinity of the phase transition temperature, and the phase transition temperature shifted to the low temperature side with increasing the number of STO coatings. This is because the phase transition temperature of KTN/STO specimen decreased with increasing the number of coatings of paraelectric STO thin film. As the applied field increases, the saturation polarization in the ferroelectric phase showed a constant value, while the induced polarization in paraelectric phase region tends to increase.

Fig. 6 shows electrocaloric temperature change ΔT of KTN/STO thin films according to the number of STO coatings. The temperature change ΔT of the thin films was calculated from the slope beginning with a maximum field and ending at a zero field as shown in Fig. 5, and the following equation [15].

$$\Delta T = -\int_{E_1}^{E_2} \frac{T}{C\rho}\left(\frac{\partial P}{\partial T}\right)_E dE \qquad (2)$$

Here, specific heat(C) and theoretical density(ρ) of the KTN thin film were 430 J/KgK and 6.231 g/cm^3, respectively [16].

Temperature change ΔT depends on the heat capacity and density of the thin film and the rate of change of the polarization depending on the temperature. All KTN/STO films showed the best ΔT properties in the temperature range of 60-80 ºC. This is because the polarization is sensitive to the thermal energy in the phase transition temperature transition to ferroelectric phase. It is believed that the polarization is sensitive to the thermal energy in the transition temperature range that transition from ferroelectric phase to paraelectric phase. The single KTN thin films exhibited the highest ΔT value, and ΔT of KTN/STO films tended to increase with increasing number of STO coatings. This is because the heat capacity (C = 102 $JKg^{-1}K^{-1}$) [17] and density (ρ = 5.11 gcm^{-3}) of STO materials are smaller than STO materials (C = 403$JKg^{-1}K^{-1}$, ρ = 6.23 gcm^{-3}), as shown in Eq. (2). Therefore, it has been observed that the temperature change ΔT can be controlled by the double layer structure thin films using materials having a high rate of change of polarization to temperature or low density and heat capacity properties. As the applied electric field increases, the ΔT increases, which is probably due to the increase of the induced polarization depending on the electric field application [18].

Conclusions

All KTN/STO thin films showed polycrystalline KTN diffraction peaks and pyrochlore phases. And no dependence on the number of coatings of STO and pyrochlore phase was observed. It was observed that the lower STO film affected upper KTN film crystallization. Dielectric constant of double layer structure KTN/STO films is higher than the value calculated by Maxwell's relation. This is probably due to the formation of a second phase between the KTN and STO films. The dependence of remanent polarization on the number of coatings of STO was not observed. It is considered that when ferroelectric phase and paraelectric phase are mutually bonded, the dipole moment of paraelectric phase is rearrangement by the ferroelectric phase dipoles. Electrocaloric temperature change ΔT showed the maximum value in the phase transition temperature range.

Acknowldgements

This research was supported by Basic Science Research Program through the National Research Foundation of Korea (NRF) funded by the Ministry of Education (No. 2017R1D1A3 B03032164).

References

1. V.K. Pecharsky, K.A. Gschneidner, Jr. Phys. Rev. Lett. 78 (1997) 4494.
2. J.H. Qiu, Q. Jiang, J. Appl. Phys. 103 (2008) 084105.
3. S. Lu, Q. Zhang, J. Adv. Dielectrics 2 (2012) 1230011.
4. A. Nazeri, M. Kahn, J. Am. Ceram. Soc. 75 (1992) 2125-2133.
5. R. Pattnaik, J. Toulouse, Phys. Rev. Lett. 79 (1997) 4677.
6. J.Y. Wang, Q.C. Guan, J.Q. Wei, Y.G. Liu, J. Cryst. Growth 116 (1992) 27.
7. H. Bae, J. Koo, J. Hong, J. Elec. Eng. Tech., 1 (2006) 120-126.
8. W. Yang, Z. Zhou, B. Yang, Y. Jiang, H. Tian, D. Gong, H. Sun, W. Chen, Appl. Surf. Sci. 257 (2011) 7221-7225.
9. C.J. Liu, A.X. Kuang, J. Mat. Sci. 32 (1997) 4421-4427.
10. D. Bao, H. Gu, A. Kuang, Ferroelectrics 188 (1996) 73-79.
11. B. Jaffe, W.R. Cook and H. Jaffe, Piezoelectric Ceramics, Academic Press, p.202.
12. R.E. Newnham, Mat. Res. Bull. 13 (1978) 525-536.
13. S. Jo, S. Lee, Y. Lee, Nanoscale Research Letters (2012) 7:54.
14. T. Katayama, W. Sakamoto, I. Yuitoo, T. Takeuchi, K. Hayashi, T. Yogo, Jap. J. Appl. Phys. 54 (2015) 10NA05.
15. B.A. Tuttle, Thesis, University of Illinois at Urbana-Champaign (1981).
16. H. Maiwa, Jpn. J. Appl. Phys. 55 (2016) 10TB09.
17. L. Feng, T. Shiga, J. Shiomi, Appl. Phys. Express 8 (2015) 071501.
18. Y. Bai, X. Han, K. Ding, and L. Qiao, Appl. Phys. Lett. 103 (2013) 162902.